RESEARCH PAPER

Investigating the Structural, Optical and Antibacterial Properties of Go, Go: Ag, GO: ZnO Thin Layers and Go: ZnO/ GO: Ag Bilayers Synthesized by Spray Pyrolysis Method

S. M. Alduwaib[1*] and M. M. Abd[2]

** Salmansur1975@gmail.com*

Received: June 2020 Revised: October 2020 Accepted: November 2020

1Department of Sciences, Collage of Basic Education, Al-Mustansiriyh University, Baghdad Iraq
2Mustansiriyah University, Collage of Basic Education, Department of Science, Baghdad Iraq

DOI: 10.22068/ijmse.17.4.170

Abstract: *Graphene oxide thin layers, graphene oxide:silver nano-composite, graphene oxide:zinc oxide nano-composite and graphene oxide:zinc oxide/graphene oxide:silver bilayer were deposited by spray pyrolysis method. The synthesized thin layers were characterized using X-ray diffraction spectroscopy, field emission scanning electron microscope, energy dispersive x-ray spectroscopy and Raman spectroscopy. The optical properties and the band gap of the thin layers were also studied and calculated using the Tauc equation. Gram-negative bacterium of Escherichia coli was used to study the antibacterial properties of thin layers. The results showed that among the thin layers investigated, GO:ZnO/GO:Ag bilayer had the greatest effect on the inhibition of E. coli growth and was able to control the growth of bacterium after 2 hours.*

Keywords: *GO:Ag Nanocomposite, GO:ZnO Nanocomposite, Bilayer, Spray Pyrolysis, Thin Layer.*

1. INTRODUCTION

Nowadays, graphene has become one of the new hot topics in research related to materials science, physics, chemistry, and nanotechnology. Graphene is a 2D one-atom-thick carbon structure that has a structure similar to the honeycomb lattice [1-4]. Graphene oxide is an oxidized derivative of graphene that is obtained by the oxidation of graphite powder. The most common method of producing the graphene oxide is Hummers method [5-7]. This process introduces the oxygen-containing groups onto graphene oxide surface. These surface functional groups can also serve as a site for the formation and growth of metal nanoparticles, metal oxide, and semiconducting oxide. However, these nanoparticles tend to accumulate during the synthesis process, which eventually results in the loss of their properties at the nanometer level. Since graphene oxide has a large surface area, it can be used as a substrate for nanoparticles. Therefore, it prevents the accumulation of nanoparticles and allows the properties of the particles to remain at the nano level. Composition and arrangement (decoration) of graphene oxide surface with metallic nanoparticles and metal oxide such as Au, Ag, Pt, Pd, and SnO_2 or nanoparticles of semiconducting oxides such as ZnO and TiO_2 improves the performance of these materials for applications such as mechanical strength materials, biochemical and electrochemical sensors, photocatalysts, lithium-ion batteries, and solar cells [8-9].

Recently, extensive research has been done on graphene nanocomposites to increase the efficiency of photocatalysts [10], solar energy conversion [11], and strong potentials in electrochemical energy devices including lithium batteries, capacitors, and fuel cells. In addition to energy applications, graphene nanocomposites have also been used as an excellent platform for environmental applications in the detection and separation of heavy ions, pollutants and bacteria [12]. These nanocomposites contain carbon plates as the substrate on which metallic or semiconducting nanoparticles are placed and help to increase the catalytic processes [13]. In 2008, Raffi et al. conducted an experiment on the antimicrobial properties of nanoparticles. They observed the growth of Escherichia coli under different concentrations of Ag nanoparticles. These nanoparticles are converted into effective bactericide at concentrations higher than 60 [14]. Jianjiang et al. carried out a study on the fabrication of rGO:ZnO nanocomposites to increase photocatalytic activity and gas sensing

[DOI: 10.22068/ijmse.17.4.170]

property [15]. Wang et al. also investigated the antibacterial activity of rGO:ZnO nanocomposites at a high concentration of Zn [16]. However, the antibacterial activity of GO:Ag and GO:ZnO nanocomposites has not been investigated so far. According to the above-mentioned cases, we decided to investigate the antibacterial properties of thin layers of graphene oxide:silver monolayer nanocomposites, graphene oxide:zinc oxide monolayer and graphene oxide:silver/graphene oxide:zinc oxide bilayer in this research.

2. SYNTHESIS METHOD

2.1. Preparation of GO:Ag Solution

Graphene oxide colloid with the concentration of 1 mg/ml (Borhan Nanomeghyas Company, Iran) was placed in the ultrasonic for 30 minutes. 40 M (molar) silver diamine hydroxide solution was prepared by combining the ammonia, deionized water and silver nitrate. To prepare GO:Ag composite, GO solution and $Ag(NH_3)OH$ solution were mixed at a volume ratio of 2: 8 and stirred for 30 minutes. It was then stirred in the oil bath at 70-80 °C for half an hour. The final solution was washed 3 times with deionized water and prepared for spray.

2.2. Preparation of GO: ZnO Solution

Graphene oxide colloid was dispersed at the ultrasonic with the concentration of 1 mg/mL. 0.2 M hexamethylene tetramine solution was then added to the graphene oxide solution and stirred. 0.2 M zinc acetate solution was added to this solution and stirred for 15 minutes. The final solution was placed in an oil bath at 90 °C for 3 hours and then washed 3 times with deionized water and prepared for the deposition.

2.3. Preparation of Thin Layer

The glass substrates were cleaned using the ultrasonic for 30 minutes and used as substrates for the growth of nanomaterials. In order to prepare thin layers, 35 ml of each solution was sprayed using the spray pyrolysis method and the compressed air as the carrier gas. Spray conditions include the distance of nozzle of about 30-40 cm and deposition rate of 2-2.5, plate temperature of 400 °C for GO:ZnO thin layers, and 150 °C for GO:Ag.

2.4. Preparation of GO:ZnO/ GO:Ag Bilayer

35 ml of GO:ZnO solution was sprayed using the spray pyrolysis method and the compressed air as the carrier gas. Spray conditions include the distance of nozzle of about 30-40 cm and deposition rate of 2-2.5. The plate temperature was set to 400 °C, and then the GO:ZnO thin film was allowed to reach room temperature. Afterward, the GO:Ag solution was sprayed with the same conditions as before on the GO:ZnO thin film at 150 °C.

2.5. Characteristics

X-ray diffraction (XRD) device, D8 Advance Bruker YT model, was used to confirm the composite structure of the synthesized thin layers, using CuKα radiation at λ = 1.5418Å at 2θ values between 5° and 80°. Field emission scanning electron microscope (FESEM), MIRA3 TESCAN-XMU model equipped with EDX analysis, was used to investigate the surface morphology and chemical analysis of the obtained layers. Raman spectroscopy was performed by Confocal Raman Spectroscopy device, Lab Ram HR model manufactured by Horiba, Japan. The optical absorption spectrum obtained from U-3500 UV/Vis device, in the wavelength range of 200-700 nm was used for the optical characterization of these layers. In order to measure the antibacterial properties, standard gram-negative bacterium of Escherichia coli DH5 alpha (ATCC 25922) (1399PTCC) were purchased from the Iran' Scientific-Industrial Research Center. Escherichia coli bacterium and the growth medium of Muller-Hinton Broth (Merck) were used to perform the test. The sample of Escherichia coli was firstly cultured in Muller Hinton Broth medium at 37 °C for 24 hours. The adsorption rate of cell density of bacterium at 630 nm was investigated by spectrophotometer. Bacterium was prepared according to the McFarland 0.5 (equivalent to 10^8 CFU/mL) using dilution method for each sample in each iteration. GO:Ag, GO:ZnO, GO:ZnO/GO:Ag thin-layer samples were placed in contact with the bacteria in the growth medium and in an incubator at 37 °C.

3. STRUCTURAL ANALYSIS

3.1. Thermal Analysis

The thermal analysis of GO and GO:Ag thin film composite was measured by TGA under a nitrogen atmosphere. For GO and GO:Ag

[DOI: 10.22068/ijmse.17.4.170]

composite, the TGA mass loss curves show two decomposition steps (Fig. 1). The first mass loss, ascribed to the elimination of interlaminar water, is found at 50 – 120 °C, and the second, where the decomposition of the oxygen groups happen, at 140–300 °C. During this step, the largest mass loss corresponds to GO (~32%), and 5.4% for GO:Ag composite. The improvement in the thermal stability is attributed to the deoxygenation and better graphitization of the composite because of the partial reduction of GO.

The decomposition behavior of the GO:ZnO was studied by thermo gravimetric analysis (TGA) and the results are shown in Fig. 2. A major weight loss is observed at 685.47 °C effected by the complete combustion of the carbon. Further, no weight loss was observed up to 1000 °C. A major weight loss was because of GO:ZnO thin film nanocomposite.

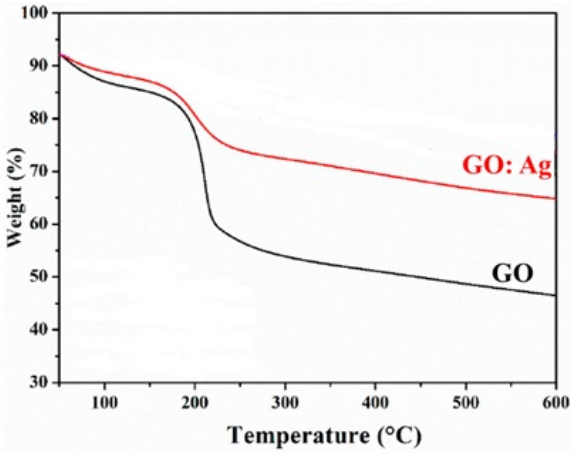

Fig. 1. TGA curves of GO and GO:Ag nano-composites.

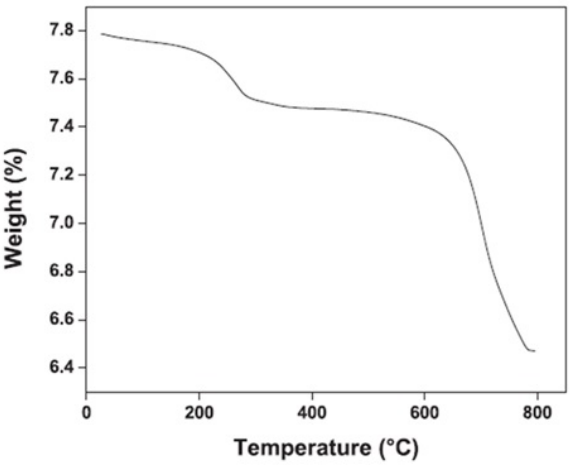

Fig. 2. TGA curves of GO:ZnO nano-composite.

3.2. XRD

XRD method is used to analyze the strucrure of the samples. Fig. 3 indicates the X-ray diffraction (XRD) spectrum for graphene oxide thin layers, GO:Ag, GO:ZnO composite and GO:ZnO/GO:Ag bilayer. Peak (002) at about 10.58 (2θ) is shown in Fig. 3a after the chemical modification of graphite using the improved method to obtain the GO. Further analysis shows that D (002) is equal to 0.4 nm. It is clear that the measured values are because of the graphene oxide presence on the substrate surface [17-18] and the intensity values indicate that a few layers of graphene oxide are formed on the substrate. Graphene oxide peak in GO:ZnO thin layer and GO:Ag/GO:ZnO bilayer almost disappeared, and the broad diffraction peak appeared at the 2θ angle of 25, related to the (002) plane of the reduced graphene oxide (rGO) layers. In addition to the peaks of graphene oxide and reduced graphene oxide, additional diffraction peaks in XRD spectrum at the 2θ angles of 38, 44.1, 64.3, and 77.3, are seen in Fig. 3c, that are related to the planes of (111), (200), (220), and (311), and represents the fcc cubic structure of pure Ag (JCPDS file no. 04-0783). XRD pattern of GO:ZnO thin layer is shown in Fig. 3b. Very small diffraction peaks for the ZnO layer with the planes of (100), (002), (101), (102), (110), (103), and (112) can be seen, that correspond with standard data for wurtzite structure of ZnO (JCPDS 36-1451) [19]. Inset picture of Fig.3b shows the xrd peaks of zinc oxide. As shown in the Fig., the formation of graphite particles (at 2θ = 25) can be attributed to the high amount of GO in the GO:ZnO thin layer because of the accumulation of graphene sheets. Fig. 3d shows the GO:ZnO/GO:Ag bilayer, which confirms the presence of the small peak of graphene oxide, the presence of graphite, the formation of high-intensity Ag plates, and the very small peaks from the formation of wurtzite phase and the presence of ZnO.

Ravichandran, et al. [44] reported Fabrication of ZnO:Ag/GO composite thin films. Their results showed that the peak position of (101) plane is slightly shifted towards the lower angle, indicating the incorporation of Ag^{+} ion into the Zn^{2+} sites. The slight shift may be caused by the larger size of Ag ions (0.114 nm) than Zn ions (0.074 nm), which are not fully substituted for the Zn sites and probably form clusters. A

[DOI: 10.22068/ijmse.17.4.170]

change in the lattice parameters is also observed as the ionic radius of Ag^{+} is greater than that of Zn^{2+} ion.

Govindhan, et al. [45] synthesized GO/ZnO–Ag nanocomposite by a combined impregnation chemical reduction method. The XRD spectra showed that the GO/ZnO–Ag composite has three peaks at 2θ values of 38.3, 44.0, and 64.6 related to the crystal plane (1 1 1), (2 0 0), and (2 2 0) which were conformed to the JCPDS- card No:08-7059 number crystal plane.

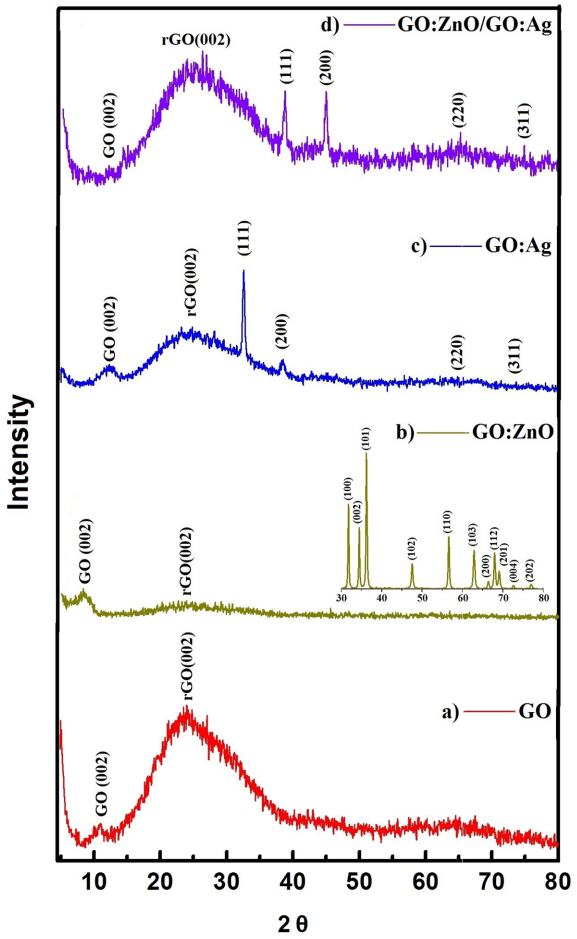

Fig. 3. X-Ray Diffraction Spectrum of a) Graphene Oxide Thin layers, b) GO:ZnO Composite (Inset: XRD pattern of ZnO peaks), c) GO:Ag and d) GO:ZnO/GO:Ag Bilayer.

3.3. FESEM Analysis

Field emission scanning electron microscope (FE-SEM) and EDX images were used to analyze the morphological aspects, size distribution, and chemical composition of pure GO and composite thin layers.

FESEM images of graphene oxide thin layers, the thin layer of GO:Ag, GO:ZnO composite and GO:ZnO/GO:Ag composite bilayer are shown in Fig. 4. Single layer of graphene oxide can be seen in Fig. 4d. Graphene oxide sheets have a relatively large surface and are well identified. 3D intertwined sheets of graphene oxide form a porous lattice which resembles the structure of a loose sponge-like with an approximate size of 49.38 nm [20].

FE-SEM images of GO:Ag thin-layer composite not only confirm the results of XRD spectroscopy, but also show that the Ag nanoparticles are heterogeneously formed. Different sizes and shapes of Ag nanoparticles, such as polyhedral and spherical shape are clear on the GO surface which can be observed in the Fig. As shown in the Fig.4, the accumulated Ag nanoparticles are randomly accumulated on GO sheets with an average size between 10 and 50 nm [21-22].

Fig. 4b indicates the FESEM image of the GO/ZnO thin layer. As expected, the structure of this composite is crust-like after reaction in the presence of GO, given the 3D cross-sectional nature of ZnO particles, which tends to homogeneously precipitate on the surface of GO sheets. The average size of the almost spherical nanoparticles of ZnO on GO sheets is between 10 to 30 nm. FESEM images of graphene oxide composite in the presence of ZnO and Ag nanoparticles show the good uniformity (Fig. 4c). The uniformity of the almost spherical nanoparticles of ZnO and Ag is large enough to completely cover the graphene oxide sheets, with particle sizes between 5 to 80 nm.

FESEM cross-section image in Fig. 5 illustrates the thickness of GO thin layer at the nanometer scale. Fig. 5a also shows the cross-section image of GO:ZnO/GO:Ag bilayer, and as can be seen in the Fig., the thickness of each layer is about 50-100 nm. The accumulation of the GO:ZnO layer is well seen in the upper layer.

The chemical compositions of GO thin layer and GO:ZnO/GO:Ag bilayer were analyzed using energy dispersive x-ray spectroscopy (EDS) and are shown in Fig. 6. The presence of C and O elements was confirmed for the graphene oxide layer and elements such as Ag and Zn in the bilayer composite sample. In this Fig., some peaks are observed which refer to platinum (Pt), Aluminium (Al) and chromium (Cr). These peaks originated from a coating which applied during the process of testing the FESEM image.

[DOI: 10.22068/ijmse.17.4.170]

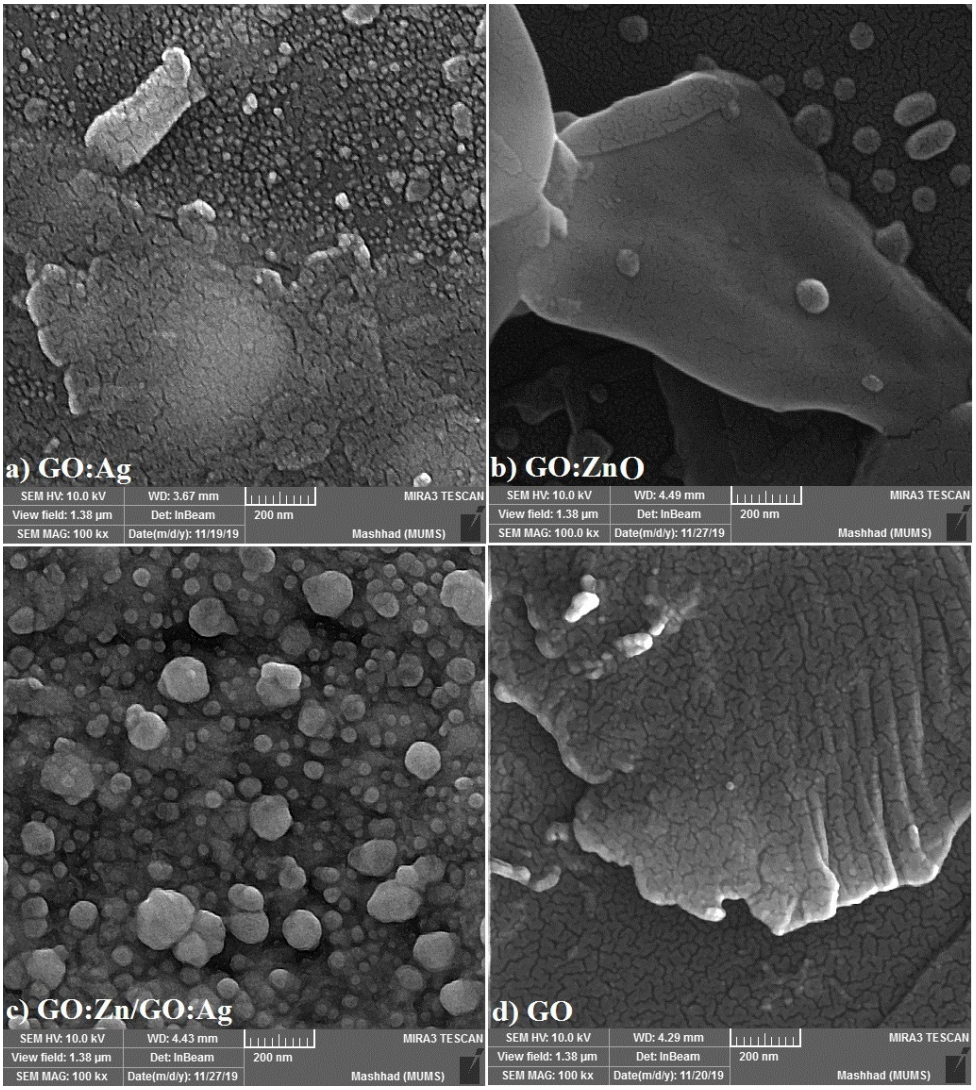

Fig. 4. FESEM Images of Graphene Oxide Thin Layers, GO:Ag, GO:ZnO Composite and GO:ZnO/GO:Ag Bilayer

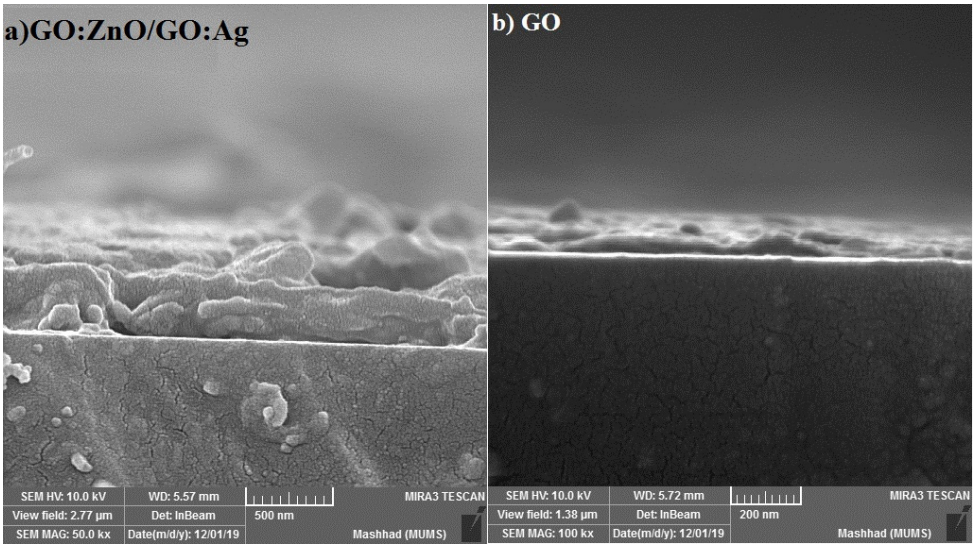

Fig. 5. FESEM Cross-Section Image of Graphene Oxide Thin Layer and GO:ZnO/GO:Ag Bilayer

[DOI: 10.22068/ijmse.17.4.170]

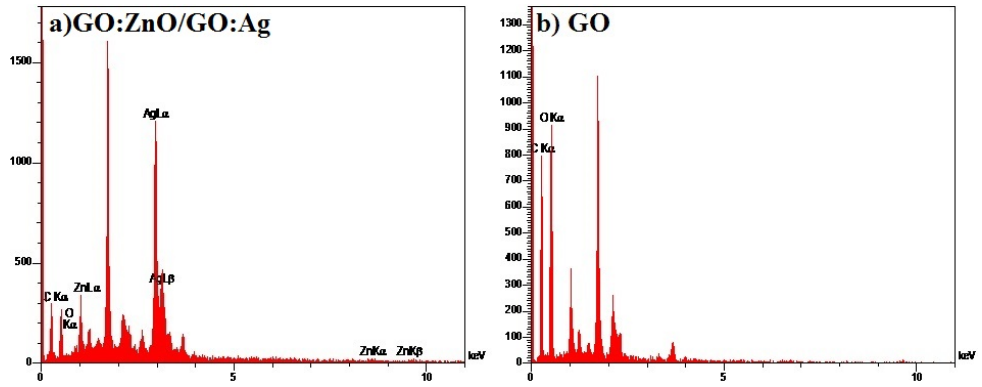

Fig. 6. Energy-Dispersive X-Ray Spectrum of Graphene Oxide Thin Layer and GO:ZnO/GO:Ag Bilayer

3.4. Raman Spectrum

Raman spectroscopy is a multipurpose technique for describing the graphene structures. Raman spectrum of the thin layer samples is plotted in Fig. 7. Graphene has two peaks, G and D. G peak at 1598cm^{-1} is related to the vibrational mode of E_{2g} of sp^2 bond of carbon atoms. Peak D at 1361cm^{-1} is related to the A_{1g} symmetric mode, containing phonons near the k-region boundary which is prohibited in graphite structure and only seen in the structural defect and disorder. The ratio of I_D/I_G intensities indicates the degree of disorder and the size of sp^2 domains. This higher ratio indicates the smaller size but the greater number of plate in the sp^2 domain [23]. Comparing the Raman spectra of two sample of GO, GO:Ag thin layer shows that G and D bands in GO:Ag, GO:ZnO, and GO:ZnO/GO:Ag samples have decreased to (1207, 1574), (1332, 1596), and (1336, 1586), respectively. This change is because of a decrease in GO during the synthesis process. The intensity of G and D peaks in GO:ZnO/GO:Ag and GO:Ag thin-layer samples increased, compared to GO sample which is caused by the effect of the increased surface scattering of Ag nanoparticles. Fig. 7 b shows the Raman spectrum of GO:ZnO thin layer and GO:ZnO/GO:Ag bilayer in the range of 300-600cm^{-1}. Two peaks are seen at 450 cm^{-1} and 544 cm^{-1} which are related to E2 ZnO and A1 longitudinal optical (LO) modes, respectively. The vibrational mode of E2 at 450 cm^{-1} is a characteristic of the wurtzite phase. Compared to other peaks, the higher intensity of E2 mode also indicates that ZnO thin layer has a well-crystallized hexagonal wurtzite structure. A1 mode at 544cm^{-1} results from the structural defects such as oxygen vacancies and Zn interstitials, and its low intensity indicates that the structural defect density is relatively low [24].

Ravichandran, et al. [44] observed a higher value of I_D/I_G ratio of ZnO/GO:Ag sample, and they reported that it may be because of an increase of smaller sp^2 domains of carbon atoms caused by the Ag addition into the ZnO/GO composite.

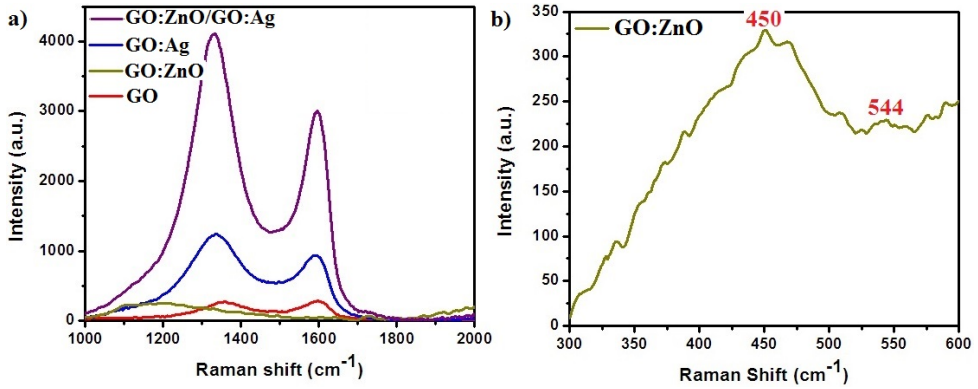

Fig. 7. a) Raman Spectrum of GO, GO:Ag, GO:ZnO, GO:ZnO/GO:Ag Thin Layers in the Range of 1000-2000cm^{-1} and b) Raman Spectrum of GO:ZnO Thin Layer in the Range 300-600 cm^{-1}.

[DOI: 10.22068/ijmse.17.4.170]

3.5. Optical Characterization

UV-Vis spectrum of GO, GO:Ag, and GO:ZnO thin layers and GO:ZnO/GO:Ag composite bilayer are shown in Fig. 8. GO thin layer (Fig. 8a) is allocated to two different bonds, one at 230 nm, related to π–π^* electronic transition of C = C aromatic bond, and a shadow shoulder at 305 nm, related to the n = π * bond of O = C [25]. Besides, Fig. 8b indicates a bonded GO:Ag thin layer at 400 nm in the absorption spectrum, which is attributed to the surface plasmon. It also shows the bond specified in GO and confirms the formation of GO/Ag thin-layer nanocomposites. The optical absorption of the GO:ZnO thin layer is shown in Fig. 8c. Given the absorption spectrum of ZnO, it is clear that the absorption spectrum shifts from the UV to the visible light region. For GO:ZnO/ GO:Ag composite bilayers, this absorption spectrum shift to the visible light region is also seen (Fig. 8d).

Optical transmission reflects the GO thin layer in the visible light range. The optical transmission of graphene oxide thin layers is in the range of 95% to 99% in the visible spectrum and the wavelength of 350 to 700 nm. The optical transmission spectrum of GO:Ag thin layer is seen in the range of 500-800 nm between 50-80% in Fig. 9. This Fig. shows the optical transmission spectrum for GO:ZnO thin layer. As can be seen, in this thin layer in the range of 350 to 800 nm, high optical transmittance is in the range of 82-85% [26].

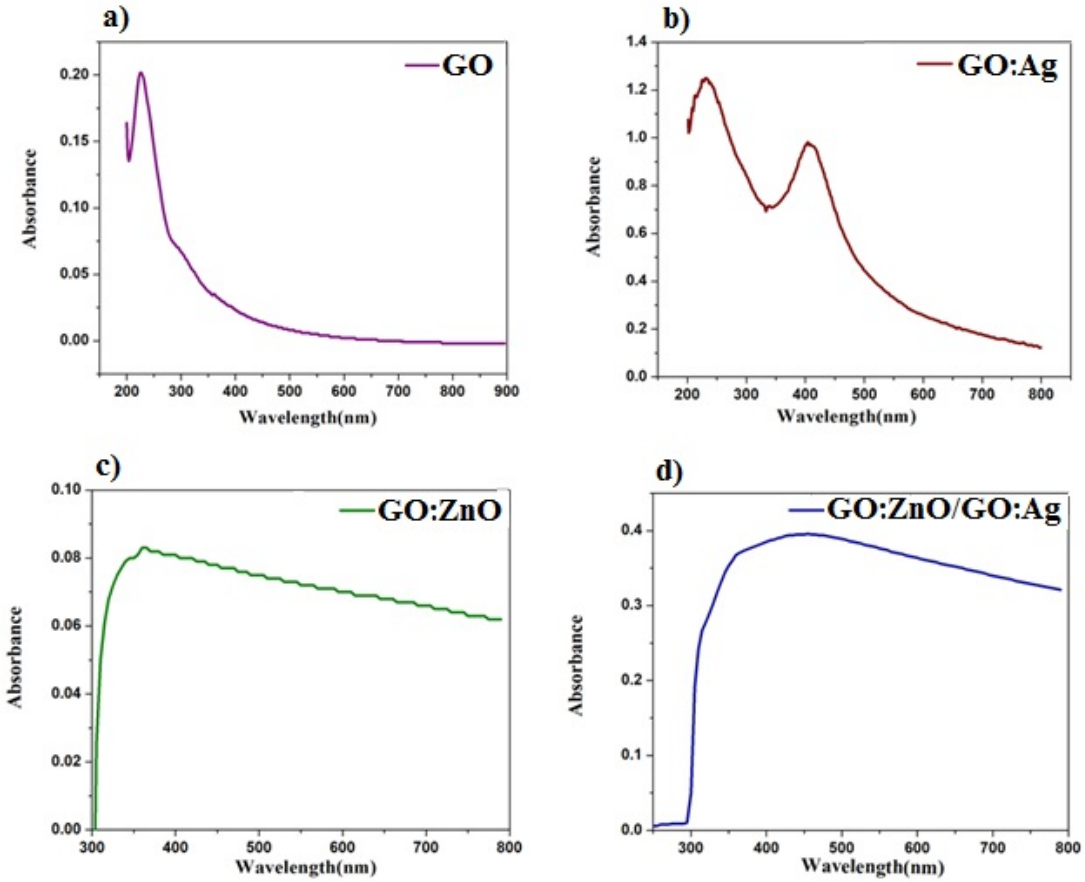

Fig. 8. UV-Vis Spectrum of GO Thin Layer, GO:Ag, GO:ZnO Thin Layers and GO:ZnO/GO:Ag Composite Bilayer

[DOI: 10.22068/ijmse.17.4.170]

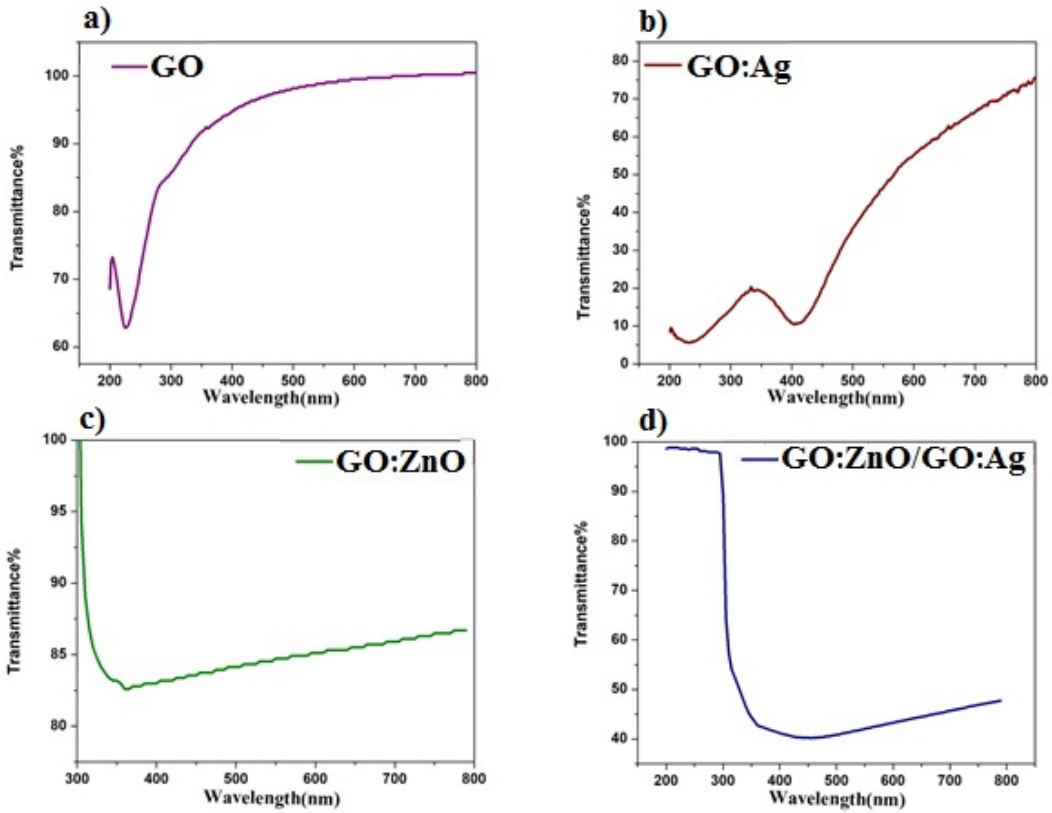

Fig. 9. Optical Transmission of a) Graphene Oxide Thin Layers, b) GO:Ag, c) GO:ZnO Thin Layers and d) GO:ZnO/GO:Ag Composite Bilayer

The pure ZnO transmission spectrum shows the high transparency (96-98%) in the visible region [27]. However, in GO:ZnO thin-layer nanocomposite, the absorption rate in the visible region increases in the presence of graphene oxide, which reduces the optical transmittance. The absorption edge was observed at about 375 nm, and this was in agreement with the studies of Karakayaetal [28] and Wineretal [29]. This strong absorption is related to the band gap, where the photons provide enough energy to create the electronic excitation across the band gap. [28]. By placing this layer on GO:Ag thin layer and forming the bilayer, the optical transmission is greatly reduced and reaches about 40% that results from the high absorption in the presence of graphene oxide.

The optical absorption coefficient (α) in the strong absorption region is calculated using the Beer-Lambert law and is shown in Equation 1.

$$\alpha=1/t*\ln(1/T) \quad (1)$$

Where, t and T are the thickness and transmittance of the layer, respectively. The band gap energy (E_g) was estimated in the high adsorption region by assuming a direct transition between the valence and conduction bands using the Tauc model (Equation 2) [30]:

$$(\alpha h\nu)^2=B(h\nu-E_g) \quad (2)$$

Where, hν is the photon energy occurred and B is an energy-independent constant. E_g for GO thin layer, GO:Ag, GO:ZnO thin layers and GO:ZnO/GO:Ag bilayer are shown in Fig. 10. E_g values are obtained by intercepting the horizontal axis by the best connections using the Tauc equation. As shown in the Fig., in graphene oxide thin layer, the band gap of 4.5eV was obtained which is in agreement with Zheng's work [31]. As observed in other studies, the band gap energy is 3.1eV for ZnO thin layer [32]. When the particles are placed on graphene oxide nanosheets, the band gap is reduced to 1.7eV. This decrease in the band gap of GO:ZnO thin layer may be related to the small size of ZnO particles, their 2D order and their less accumulated structure on GO nanoparticles. The band gap energy is about 3.7eV for GO:Ag thin layer and about 1.4eV for GO:ZnO/GO:Ag bilayer.

[DOI: 10.22068/ijmse.17.4.170]

3.6. Antibacterial Properties

The antibacterial effect of thin layers on Escherichia coli was investigated according to CLSL international standard with three iterations using micro-dilution method. The absorption rate of samples was read in ELISA Reader after 0, 2, 4, and 20 hours of incubation at 37 °C. The mean of the different iterations was calculated and plotted for each sample at different times. The absorption rate of samples was compared with positive and negative control, to investigate the effect of thin layers on E. coli. The results are plotted in Fig. 11 and showed that among the thin layers investigated, GO:ZnO/GO:Ag bilayer had the greatest effect on the inhibition of E. coli growth and was able to control the bacterial growth even after 2 hours. GO:Ag sample was also able to control the growth of bacterium after 2 hours, but GO:ZnO thin layer has failed to inhibit E. coli growth. Many researchers have investigated the antibacterial properties of graphene oxide plates in the presence of different nanoparticles. The mechanism of the antibacterial activity of the graphene oxide plates is that GO plates interact with the cell membrane, and the accumulation of cell-GO is formed, which eventually results in disruption and degradation of the cell membrane. The particle size and the type of functional groups present on the surface of GO plates are the main factors that influence the antibacterial activity of GO [33-38]. However, the mechanism of antibacterial activity of Ag nanoparticles has not been fully determined yet. Recent studies show that nanoparticles have more effective antibacterial activity than their bulk samples. Factors affecting the antibacterial activity of Ag nanoparticles include particle size, high dispersion, and strong adhesion between metal and carbon in graphene oxide plates [39-40]. The results of the researchers' reports show that Ag/graphene nanocomposites exhibit strong antibacterial activity against the gram-positive bacterium of Staphylococcus Aureus and gram-negative bacterium of E. coli [41-42]. Franklin et al. concluded that the solubility rate of ZnO is an important factor in the antibacterial activity of ZnO, and it has a good antibacterial activity at concentrations higher than 10 mg/mL but does not have good antibacterial activity at low concentrations [43]. In the research, as shown in XRD images, ZnO concentration is very low so it cannot inhibit E. coli growth.

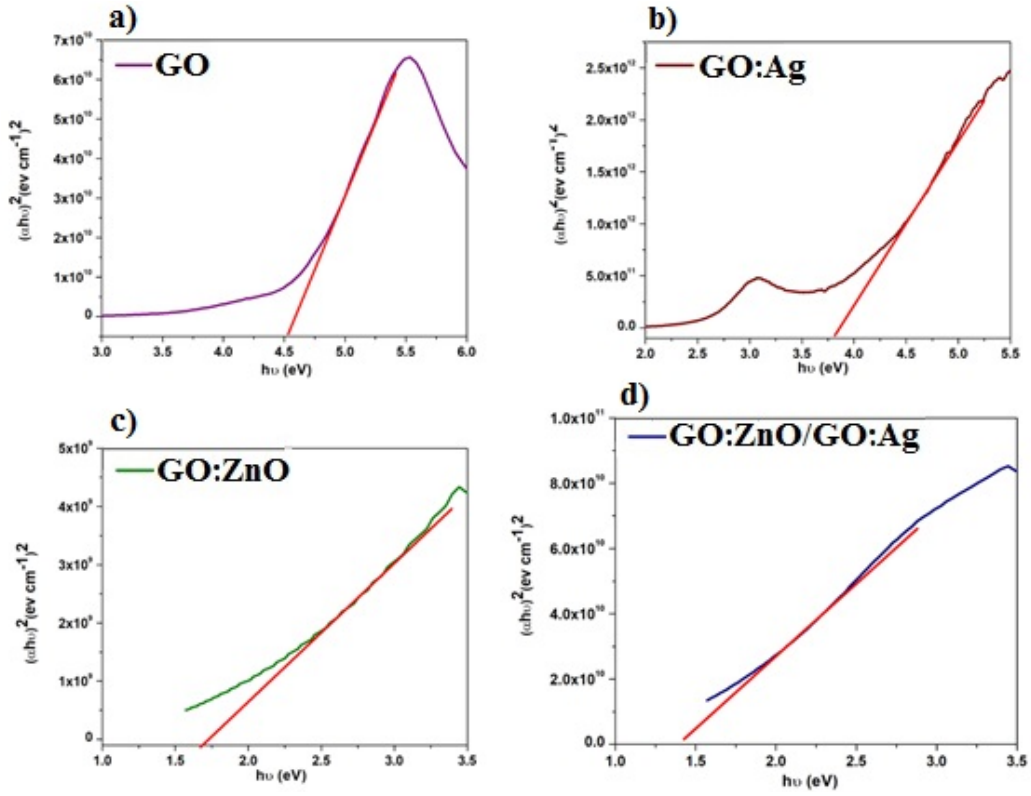

Fig. 10. Calculation of Optical Band Gap for a) GO Thin Layer, b) GO:Ag, c) GO:ZnO Thin Layers and d) GO:ZnO/GO:Ag Bilayers Using the Tauc Equation

[DOI: 10.22068/ijmse.17.4.170]

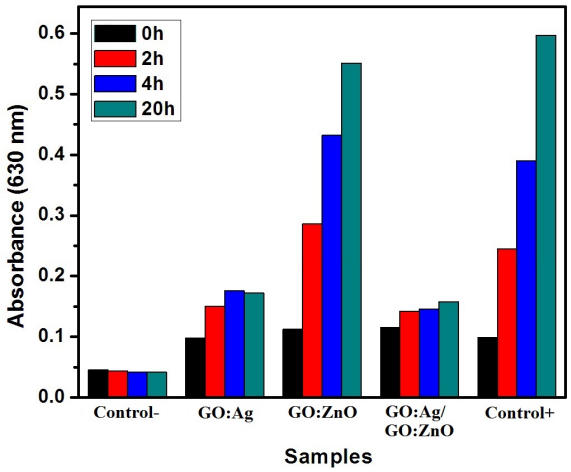

Fig. 11. Investigation of the Antibacterial Effect of GO:Ag, GO:ZnO, GO:ZnO/GO:Ag Thin-Layer Sample on E. Coli

4. CONCLUSION

Graphene oxide thin layers, GO:Ag nanocomposite, GO:ZnO nanocomposite, and GO:ZnO/GO:Ag bilayer were deposited by spray pyrolysis method. The analysis of x-ray diffraction spectrum and the investigation of field emission scanning electron microscope images confirm the formation of the given thin layers. Comparing the Raman spectra of GO thin layer with GO:Ag, GO:ZnO, and GO:ZnO/GO:Ag samples shows that when GO is reduced during the synthesis process, the ID/IG will change**.** The optical properties and the band gap of the thin layers were also studied and calculated using the Tauc equation. The amount of band gap of graphene oxide thin layer of 4.5eV is obtained. According to other reports, the band gap energy of ZnO thin layer is equal to 3.1eV. When the particles are placed on graphene oxide nanosheets, the amount of band gap is reduced to 1.7eV. This decrease in the band gap of GO:ZnO thin layer may be caused by the small size of ZnO particles, their 2D order, and their less accumulated structure on GO nanoparticles. The band gap energy is about 3.7eV for GO:Ag thin layer and about 1.4eV for GO:ZnO/GO:Ag bilayer. Gram-negative bacterium of Escherichia coli was used to study the antibacterial properties of the thin layers. The results showed that GO:ZnO/GO:Ag bilayer had the greatest effect on the inhibition of E. coli growth and were able to control the growth of bacterium after 2 hours. GO:Ag sample was also able to control the growth of bacterium after 2 hours, but GO:ZnO thin layer was unable to inhibit E. coli growth due to the very low concentration of ZnO.

REFERENCES

1. W. Choi, J.-w. Lee, Graphene: synthesis and applications, CRC Press, 2011, 263-89.
2. Shohany BG, Roknabadi MR, Kompany A, "DFT-NEGF simulation of graphene-graphdiyne-graphene resonant tunneling transistor." Computational Materials Science, 2018, 144, 280-284.
3. Shohany BG, Roknabadi MR, Kompany A, "Electrical investigation of armchair graphene-graphdiyne-graphene nanoribbons heterojunctions." Communications in Theoretical Physics, 2016, 65, 99-104.
4. Wang Y, Li Z, Wang J, Li J, Lin Y, "Graphene and graphene oxide: biofunctionalization and applications in biotechnology." Trends in biotechnology, 2011, 29, 205-212.
5. Wei J, Vo T, Inam F, "Epoxy/graphene nanocomposites–processing and properties: a review." RSC Advances, 2015, 5, 73510-73524.
6. Skákalová, V, and Kaiser, A B, Graphene: properties, preparation, characterisation and devices, Woodhead Publishing, UK, 2014, 350-379.
7. Zhou X, Shi T, Zhou H, "Hydrothermal preparation of ZnO-reduced graphene oxide hybrid with high performance in photocatalytic degradation." Applied surface science, 2012, 258, 6204-6211.
8. Motevalizadeh L, Shohany BG, Abrishami ME, "Effects of Mn doping on electrical properties of ZnO thin films." Modern Physics Letters B., 2016, 30(04), 1650024:1-12.
9. Zhao J, Liu L, Li F, Graphene oxide: physics and applications, Springer, UK, 2015, 54-67.
10. Li D, Müller MB, Gilje S, Kaner RB, Wallace GG., "Processable aqueous dispersions of graphene nanosheets." Nature nanotechnology, 2008, 3(2), 101-105.
11. Tian J, Liu S, Zhang Y, Li H, Wang L, Luo Y, Asiri AM, Al-Youbi AO, Sun X., "Environmentally friendly, one-pot synthesis of Ag nanoparticle-decorated reduced graphene oxide composites and their application to photocurrent generation." Inorganic chemistry, 2012, 51(8), 4742-4746.

[DOI: 10.22068/ijmse.17.4.170]

12. Chang H, Wu H., "Graphene-based nanocomposites: preparation, functionalization, and energy and environmental applications." Energy & Environmental Science, 2013, 6(12), 1-23.
13. Williams G, Seger B, Kamat PV, "TiO2-graphene nanocomposites. UV-assisted photocatalytic reduction of graphene oxide." ACS nano., 2008, 2(7), 1487-1491.
14. Raffi M, Hussain F, Bhatti TM, Akhter JI, Hameed A, Hasan MM, "Antibacterial characterization of silver nanoparticles against E. coli ATCC-15224." Journal of materials science and technology, 2008, 24(2), 192-196.
15. He J, Niu C, Yang C, Wang J, Su X, "Reduced graphene oxide anchored with zinc oxide nanoparticles with enhanced photocatalytic activity and gas sensing properties." RSC Advances, 2014, 4(104), 60253-60259.
16. Wang YW, Cao A, Jiang Y, Zhang X, Liu JH, Liu Y, Wang H, "Superior antibacterial activity of zinc oxide/graphene oxide composites originating from high zinc concentration localized around bacteria." ACS applied materials & interfaces, 2014, 6(4), 2791-2798.
17. Ali H. A. Jalaukan, Salah aldin M. Aldowaib, Ammar S. Hameed, Boshra Ghanbari Shohany, Reihaneh Etefagh, Ali Khorsand Zak, "Photo catalytic Activity, Antibacterial Effect, and Self Cleaning properties of TiO2/GO thin films", Iranian Journal of Materials Science and Engineering, 2019, 16, 53-62.
18. Ji L, Wu Y, Ma L, Yang X, "Noncovalent functionalization of graphene with pyrene-terminated liquid crystalline polymer." Composites Part A: Applied Science and Manufacturing, 2015, 72, 32-39.[19] Shohany BG, Motevalizadeh L, Abrishami ME, "Investigation of ZnO thin-film sensing properties for CO2 detection: effect of Mn doping." Journal of Theoretical and Applied Physics, 2018, 12(3), 219-225.
19. Islami M, Zarrabi A, Tada S, Kawamoto M, Isoshima T, Ito Y, "Controlled quercetin release from high-capacity-loading hyperbranched polyglycerol-functionalized graphene oxide." International journal of nanomedicine, 2018, 13, 6059-6071.
20. Shao W, Liu X, Min H, Dong G, Feng Q, Zuo S, "Preparation, characterization, and antibacterial activity of silver nanoparticle-decorated graphene oxide nanocomposite." ACS applied materials & interfaces, 2015, 7(12), 6966-6973.
21. De Faria AF, Martinez DS, Meira SM, de Moraes AC, Brandelli A, Souza Filho AG, Alves OL, "Anti-adhesion and antibacterial activity of silver nanoparticles supported on graphene oxide sheets." Colloids and Surfaces B: Biointerfaces, 2014, 113, 115-124.
22. Ferrari AC, Robertson J, "Interpretation of Raman spectra of disordered and amorphous carbon." Physical Review B, 2000, 61, 14095 - 14107.
23. Ghanbari Shohany B, Khorsand Zak A, "Doped ZnO nanostructures with selected elements—structural, morphology and optical properties: a review" Ceramics International, 2020, 46(5), 5507-5520.
24. Stobinski L, Lesiak B, Malolepszy A, Mazurkiewicz M, Mierzwa B, Zemek J, Jiricek P, Bieloshapka I, "Graphene oxide and reduced graphene oxide studied by the XRD, TEM and electron spectroscopy methods." Journal of Electron Spectroscopy and Related Phenomena, 2014, 195, 145-154.
25. Shinde SS, Shinde PS, Oh YW, Haranath D, Bhosale CH, Rajpure KY, "Structural, optoelectronic, luminescence and thermal properties of Ga-doped zinc oxide thin films." Applied Surface Science, 2012, 258(24), 9969-9976.
26. Muchuweni E, Sathiaraj TS, Nyakotyo H, "Synthesis and characterization of zinc oxide thin films for optoelectronic applications." Heliyon, 2017, 3(4), e00285.
27. Karakaya S, Ozbas O, "Preparation and Characterization of Highly Conducting and Transparent ZnO Thin Films by Ultrasonic Spray Pyrolysis." Canadian Journal of Basic and Applied Sciences, 2015, 3(2), 53-58.
28. Winer I, Shter GE, Mann-Lahav M, Grader GS, "Effect of solvents and stabilizers on sol-gel deposition of Ga-doped zinc oxide TCO films." Journal of Materials Research, 2011, 26(10), 1309-1315.
29. Tauc J, Grigorovici R, Vancu A, "Optical properties and electronic structure of amorphous germanium." Physica Status Solidi (b), 1966, 15(2), 627-637.

[DOI: 10.22068/ijmse.17.4.170]

30. Zheng F, Xu WL, Jin HD, Hao XT, Ghiggino KP, "Charge transfer from poly (3-hexylthiophene) to graphene oxide and reduced graphene oxide." RSC Adv., 2015, 5, 89515-89520.
31. Oktik S, "Low cost, non-vacuum techniques for the preparation of thin/thick films for photovoltaic applications." Progress in Crystal Growth and Characterization, 1988, 17(3), 171-240.
32. Dizaj SM, Mennati A, Jafari S, Khezri K, Adibkia K, "Antimicrobial activity of carbon-based nanoparticles." Advanced Pharmaceutical Bulletin, 2015, 5(1), 19-23.
33. Gurunathan S, Han JW, Dayem AA, Eppakayala V, Kim JH, "Oxidative stress-mediated antibacterial activity of graphene oxide and reduced graphene oxide in Pseudomonas aeruginosa." International Journal of Nanomedicine, 2012, 7, 5901-5914.
34. Dinadayalane TC, Leszczynska D, Leszczynski J, Towards Efficient Designing of Safe Nanomaterials, ed. Leszczynski J, Puzyn T, Kroto H, UK, 2012, 69-112.
35. Yang K, Wan J, Zhang S, Zhang Y, Lee ST, Liu Z, "In vivo pharmacokinetics, long-term biodistribution, and toxicology of PEGylated graphene in mice." ACS nano., 2011, 5(1), 516-522.
36. Lu Z, Dai T, Huang L, Kurup DB, Tegos GP, Jahnke A, Wharton T, Hamblin MR, "Photodynamic therapy with a cationic functionalized fullerene rescues mice from fatal wound infections." Nanomedicine (Lond), 2010, 5(10), 1525-1533.
37. Azimi S, Behin J, Abiri R, Rajabi L, Derakhshan AA, Karimnezhad H, "Synthesis, characterization and antibacterial activity of chlorophyllin functionalized graphene oxide nanostructures." Science of Advanced Materials, 2014, 6(4), 771-781.
38. Kim JD, Yun H, Kim GC, Lee CW, Choi HC, "Antibacterial activity and reusability of CNT-Ag and GO-Ag nanocomposites." Applied Surface Science, 2013, 283, 227-233.
39. Wang YW, Cao A, Jiang Y, Zhang X, Liu JH, Liu Y, Wang H, "Superior antibacterial activity of zinc oxide/graphene oxide composites originating from high zinc concentration localized around bacteria." ACS Applied Materials & Interfaces, 2014, 6(4), 2791-2798.
40. Tai Z, Ma H, Liu B, Yan X, Xue Q, "Facile synthesis of Ag/GNS-g-PAA nanohybrids for antimicrobial applications." Colloids and Surfaces B: Biointerfaces, 2012, 89, 147-151.
41. Das MR, Sarma RK, Saikia R, Kale VS, Shelke MV, Sengupta P, "Synthesis of silver nanoparticles in an aqueous suspension of graphene oxide sheets and its antimicrobial activity." Colloids and Surfaces B: Biointerfaces, 2011, 83(1), 16-22.
42. Franklin NM, Rogers NJ, Apte SC, Batley GE, Gadd GE, Casey PS, "Comparative Toxicity of Nanoparticulate ZnO, Bulk ZnO, and ZnCl2 to a Freshwater Microalga (Pseudokirchneriella subcapitata): The Importance of Particle Solubility." Environmental Science & Technology, 2007, 41(24), 8484-8490.
43. Ravichandran K, Uma R, Sriram S, Balamurgan D, "Fabrication of ZnO: Ag/GO composite thin films for enhanced photocatalytic activity." Ceramics International, 2017, 43(13), 10041-10051.
44. Govindhan P, Pragathiswaran C, Chinnadurai M, "Facile synthesis of GO/ZnO–Ag nanocomposite and evaluation of rhodamine B dye under sun light." Journal of Materials Science: Materials in Electronics, 2017, 28(1), 354-362.

[DOI: 10.22068/ijmse.17.4.170]